ARCHIVES OF ELECTRICAL ENGINEERING VOL. 62(2), pp. 267-279 (2013)

DOI 10.2478/aee-2013-0021

Analysis and synthesis of converter control system of autonomous induction generator with field oriented control

BŁAŻEJ JAKUBOWSKI, KRZYSZTOF PIEŃKOWSKI

Institute of Electrical Machines, Drives and Measurements
Wroclaw University of Technology
Wybrzeze Wyspianskiego 27, 50-370 Wroclaw, Poland
e-mail: {blazej.jakubowski/krzysztof.pienkowski}@pwr.wroc.pl

(Received: 17.06.2012, revised: 22.01.2013)

Abstract: The paper presents the mathematical model of an autonomous induction generator with the AC load circuit and the converter control system of the voltage magnitude at the terminals of stator generator. The control algorithm and the structure of the control system are described. The simulation results of the control system are presented and discussed.

Key words: induction generator, converter control, field oriented control, synthesis of control system

1. Introduction

Recently, there is a growing use of induction machines in power generation, especially for supplying electrical power in remote areas. The three-phase induction machine with a squirrel-cage rotor could work as an autonomous induction generator. The induction generator can operate in the self-excitation power generation mode when an appropriate capacitor bank is connected in parallel with its stator terminal ports. The operation of isolated induction generator with PWM converter excitation has been the subject of some papers [1, 5-11].

The serious problem with the isolated induction generator is its poor voltage regulation. The simple method for overcoming such problems is based on using capacitor bank with switched capacitors. This control system is simple, but the excitation capacitances must be varied over a wide range to maintain the generator voltage constant. The better method is based on using power electronics converter and field-orientation control algorithms to excite and control the voltage of the three-phase isolated induction generator. In the previous papers the isolated induction generator with PWM converter excitation and with capacitor and the load connected to DC link of converter has been considered [2, 4, 6, 9, 10]. In this paper more general system is analyzed.

The system of an autonomous induction generator with excitation control accomplished by capacitor bank with constant capacitances and an AC/DC converter connected in parallel with generator stator terminals is considered in the paper. The mathematical model of the control system is described. The control loops of the system are analyzed for the synthesis of controller parameters. On the base of the analysis and the synthesis of the considered control system, the simulation studies are performed and discussed. The aspects related to voltage regulation using field-orientation control strategy for PWM voltage source inverter are investigated and discussed.

2. The scheme and mathematical model of converter control system of autonomous induction generator

The scheme of the considered control system of an autonomous induction generator is presented in Figure 1. The three-phase induction generator is loaded by balanced three-phase AC resistive-inductive load (R_o, L_o). The capacitor bank with fixed valued excitation capacitors C is connected in parallel with the stator terminals of induction generator. The capacitor bank supplies the exciting currents required to maintain the no-load voltage of the generator at the rated value. The AC/DC converter is connected in parallel with the excitation capacitors. The converter consists of a three-phase IGBT based current controlled voltage source inverter with an electrolytic capacitor C_d at its DC link. The AC output terminals of the inverter are connected to the AC terminals of induction generator through a three-phase filter impedance (R_p, L_p).

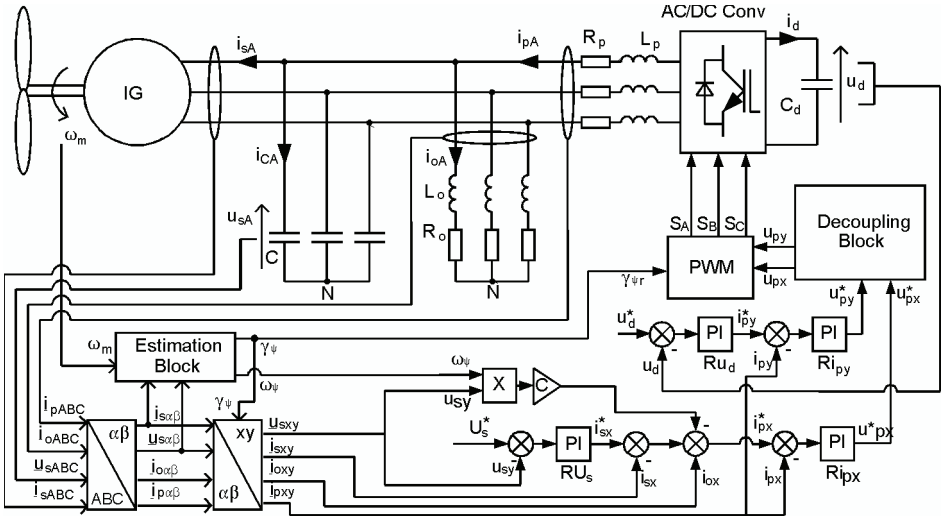

Fig. 1. The scheme of the control system of autonomous induction generator

The AC/DC converter acts as a controlled source of leading or lagging current in order to control the voltage magnitude U_s of generator stator terminals with variation of the load in the

system and to control the voltage u_d in the DC link of the converter. The principle of direct field-oriented control (DFOC) has been implemented [1]. The induction generator is controlled in a (x, y) axis frame, synchronously rotating with the d-axis oriented along the rotor-flux vector position. The magnitude and the angle position of rotor-flux vector are determined in estimation block of control system.

In order to perform the analysis and synthesis of the control structure the mathematical model of the whole system has been formulated. Since the induction generator is connected to an isolated load, the magnetizing current of the generator is not constant. The value of the magnetizing inductance should be considered as a nonlinear function of magnetizing phase current of generator. The model of induction machine including nonlinearity of main magnetic circuit has been taken into account. The cage rotor winding of induction generator is replaced by an equivalent three-phase winding. All the electromagnetic variables and parameters of the equivalent rotor winding have been transferred to the stator side. All equations of the system have been expressed in the rectangular reference frame (x, y) rotating with angular velocity ω_Ψ, synchronously with the rotor flux vector. After some manipulations the obtained system of equations has the following form:

$$\begin{cases} \underline{u}_s = R_s \underline{i}_s + \dfrac{d\underline{\Psi}_s}{dt} + j\omega_\Psi \underline{\Psi}_s \\ 0 = R_r \underline{i}_r + \dfrac{d\underline{\Psi}_r}{dt} + j(\omega_\Psi - \omega_e)\underline{\Psi}_r, \end{cases} \tag{1a}$$

$$\begin{cases} \underline{\Psi}_s = L_s \underline{i}_s + L_m \underline{i}_r \\ \underline{\Psi}_r = L_r \underline{i}_r + L_m \underline{i}_s, \end{cases} \tag{1b}$$

$$\begin{cases} |\underline{\Psi}_m| = A_m \operatorname{arctg}(B_m |\underline{i}_m|) \\ L_m = |\underline{\Psi}_m| \,/\, |\underline{i}_m| \\ \underline{i}_m = \underline{i}_s + \underline{i}_r, \end{cases} \tag{1c}$$

where: R_s, R_r – resistance of stator and rotor phase winding, respectively, $L_s = L_{s\sigma} + L_m$, $L_r = L_{r\sigma} + L_m$ – inductance of stator and rotor phase winding, respectively, L_m – magnetizing inductance, $L_{s\sigma}$, $L_{r\sigma}$ – leakage inductance of stator and rotor phase winding, respectively, $\underline{i}_s$, $\underline{i}_r$, $\underline{i}_m$ – vectors of stator, rotor and magnetizing current of generator, respectively, $\underline{u}_s$ – vector of stator voltage of generator, $\underline{\Psi}_s$, $\underline{\Psi}_r$, $\underline{\Psi}_m$ – vectors of stator, rotor and magnetizing flux of generator, respectively, A_m, B_m – coefficients of the approximation function describing nonlinearity of main magnetic path of induction generator. All the electromagnetic variables and parameters of the rotor have been transferred to the stator side.

In this model the nonlinearity of magnetizing curve of generator magnetic circuit has been taken into account through including the nonlinear dependence of the magnitude of the magnetizing flux vector Ψ_m from the magnitude of the magnetizing current vector i_m.

The system of equations, describing: the AC load circuits (2), the exciting capacitor bank (3), the DC link circuit of the converter (4), the coupling AC circuits of the converter(5), the balance of AC currents (6) and equations describing the principle of operation of AC/DC converter (7) is presented below:

$$\underline{u}_s = R_o \underline{i}_o + L_o \frac{d\underline{i}_o}{dt} + j\omega_\Psi L_o \underline{i}_o, \tag{2}$$

$$\underline{i}_C = C \frac{d\underline{u}_s}{dt} + j\omega_\Psi C \underline{u}_s, \tag{3}$$

$$C_d \cdot \frac{du_d}{dt} = i_d, \tag{4}$$

$$\underline{u}_p - \underline{u}_s = R_p \underline{i}_p + L_p \cdot \frac{d\underline{i}_p}{dt} + j\omega_\Psi L_p \underline{i}_p, \tag{5}$$

$$\underline{i}_p = \underline{i}_o + \underline{i}_C + \underline{i}_s, \tag{6}$$

$$i_d = -\left(S_A\, i_{pA} + S_B\, i_{pB} + S_C\, i_{pC}\right), \tag{7a}$$

$$u_{pk} = (1/3) \cdot \left[3S_k - \left(S_A + S_B + S_C\right)\right] \cdot u_d, \tag{7b}$$

where: $\underline{u}_\mathrm{p}$ – space vector of AC/DC converter voltage, u_{pk} – value of voltage in phase k in AC circuit of converter, u_d, i_d – value of voltage and current in DC circuit of converter, $\underline{i}_\mathrm{p}$, $\underline{i}_\mathrm{o}$, $\underline{i}_\mathrm{c}$ – the current vector of AC/DC converter, AC load and exciting bank capacitor, respectively, S_k – the logical value describing the state of k-switch of AC/DC converter, $k = A, B, C$.

3. Analysis of the control system

3.1. Current loop control of AC/DC converter

The relationship between x,y-components of the converter vector current $\underline{i}_\mathrm{p}$, and converter vector voltage $\underline{u}_\mathrm{p}$ of the AC side of the inverter in the field-oriented reference frame represent the Equations (8). In these equations there are elements that cause coupling between components of voltage space vector and components of current space vector of AC/DC converter in the axis x and y. This means that the component of the voltage space vector of converter in one axis forces the current space vector components in both axes. In order to eliminate this disadvantage, in the control system the decoupling signals $\underline{u}_\mathrm{pox}$, $\underline{u}_\mathrm{poy}$ are generated. These signals are next added to the reference components $\underline{u}_\mathrm{pxz}$, $\underline{u}_\mathrm{pyz}$ of space vector voltage of AC/DC converter (9). After substituting Equations (9) to (8) the relationship (10) is obtained. On the base of the Equations (10), it can be stated, that these operations allow to independent control of current space vector components i_{px} and i_{py}, accordingly by forcing components of voltage space vector u_{pxz} and u_{pyz}:

$$\begin{cases} u_{px} = R_p i_{px} + L_p \dfrac{di_{px}}{dt} - \omega_\Psi L_p i_{py} + u_{sx}, \\ u_{py} = R_p i_{py} + L_p \dfrac{di_{py}}{dt} + \omega_\Psi L_p i_{px} + u_{sy}, \end{cases} \tag{8}$$

$$\begin{cases} u_{px} = u_{pxz} + u_{pxo}, \\ u_{py} = u_{pyz} + u_{pyo}, \\ u_{pxo} = -\omega_\Psi L_p i_{py} + u_{sx}, \\ u_{pyo} = \omega_\Psi L_p i_{px} + u_{sy}, \end{cases} \tag{9}$$

$$\begin{cases} u_{pxz} = R_p i_{px} + L_p \dfrac{di_{px}}{dt}, \\ u_{pyz} = R_p i_{py} + L_p \dfrac{di_{py}}{dt}. \end{cases} \tag{10}$$

The Equations (10) has been applied to the synthesis of the control system of the output current of the AC/DC converter. The block structures of the control system are presented in Figure 2 (where: $K_p = 1/R_p$, $T_p = L_p/R_p$).

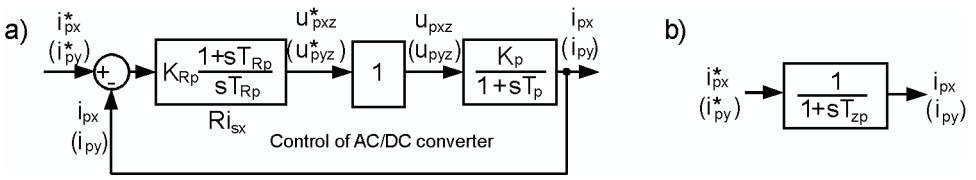

Fig. 2. The schemes of current control of inverter: a) the complete scheme, b) the scheme after compensation

In the considerations it has been assumed that the transfer function of voltage source converter is equal to unity. In order to eliminate the current deviation, the proportional-integral (PI) controller with parameters T_{Rp} and K_{Rp} has been used in the control system. The full structure of output current control system is presented in Figure 2a. By choosing the value of parameter T_{Rp} equal to T_p we can get the simple scheme of current control system as is shown in Figure 2b, where:

$$T_{zp} = \frac{T_p}{K_{Rp} K_p}. \tag{11}$$

For the data: L_p = 50 mH, R_p = 0.2 Ω we obtain the following values of the time constant of the current control system: $T_{rp} = T_p$ = 0.25 s. K_{Rp} gain factor should be tuned separately for the state variables in the x and y axes based on the control structure of the external control system i.e. control structure for voltage magnitude of generator (for axis x) and control structure for voltage in DC link of AC/DC converter (for axis y).

3.2. Control of *x*-axis current component of AC/DC converter and stator voltage magnitude of induction generator

The system of the equations (1) after some manipulation is transformed to the new form of Equations (12):

$$\frac{d}{dt}\begin{bmatrix} i_{sx} \\ i_{sy} \\ \Psi_{rx} \\ \Psi_{ry} \end{bmatrix} = \begin{bmatrix} -\dfrac{R_r L_m^2 + R_s L_r^2}{L_r(L_s L_r - L_m^2)} & \omega_\Psi & \dfrac{L_m R_r}{L_r(L_s L_r - L_m^2)} & \dfrac{\omega_e L_m}{L_s L_r - L_m^2} \\ -\omega_\psi & -\dfrac{R_r L_m^2 + R_s L_r^2}{L_r(L_s L_r - L_m^2)} & -\dfrac{\omega_e L_m}{L_s L_r - L_m^2} & \dfrac{L_m R_r}{L_r(L_s L_r - L_m^2)} \\ \dfrac{L_m R_r}{L_r} & 0 & -\dfrac{R_r}{L_r} & \omega_K - \omega_e \\ 0 & \dfrac{L_m R_r}{L_r} & -(\omega_\psi - \omega_e) & -\dfrac{R_r}{L_r} \end{bmatrix} \cdot \begin{bmatrix} i_{sx} \\ i_{sy} \\ \Psi_{rx} \\ \Psi_{ry} \end{bmatrix} + \\ + \begin{bmatrix} \dfrac{L_r}{L_s L_r - L_m^2} & 0 \\ 0 & \dfrac{L_r}{L_s L_r - L_m^2} \\ 0 & 0 \\ 0 & 0 \end{bmatrix} \cdot \begin{bmatrix} u_{sx} \\ u_{sy} \end{bmatrix}. \tag{12}$$

The state variables in the control system are considered in the common reference frame (x, y) with the x-axis aligned with the vector of rotor flux linkage. Since the Ψ_{ry} component of the rotor flux space vector is equal to zero the equation for this component can be omitted in further analysis.

On the basis of Equation (12) the relationships that describe the components u_{sx} and u_{sy} of stator voltage vector of induction generator have the following form:

$$\begin{cases} u_{sx} = \dfrac{(L_r L_s - L_m^2)}{L_r}\dfrac{d}{dt} i_{sx} + \dfrac{R_r L_m^2 + R_s L_r^2}{L_r^2} \cdot i_{sx} - \omega_\Psi \dfrac{(L_r L_s - L_m^2)}{L_r} \cdot i_{sy} - \dfrac{L_m R_r}{L_r^2} \cdot \Psi_r \\ u_{sy} = \dfrac{(L_r L_s - L_m^2)}{L_r}\dfrac{d}{dt} i_{sy} + \omega_\psi \dfrac{(L_r L_s - L_m^2)}{L_r} \cdot i_{sx} + \dfrac{R_r L_m^2 + R_s L_r^2}{L_r^2} \cdot i_{sy} + \dfrac{\omega_e L_m}{L_r} \cdot \Psi_r. \end{cases} \tag{13}$$

For a given values of parameters and electromagnetic state variables of induction generator the Equations (13) can be used for the calculation of the values of the stator voltage vector component u_{sx} and u_{sy} and the magnitude U_s of stator voltage vector of induction generator. The results of these calculations are presented in Figure 3 and in Figure 4. The worst case of operation occurs when the component i_{sx} of stator current vector is greater than zero and increases and the component i_{sy} of stator current vector is less than zero and decreases. The calculations presented in Figures 3 and 4 are performed for the following values: L_m = 0.2 H, $\mathrm{d}i_{sx}/\mathrm{d}t$ = 1000 A/s, $\mathrm{d}i_{sy}/\mathrm{d}t$ = –1000 A/s, ω_Ψ = 290 rad/s, ω_e = 300 rad/s, Ψ_{rx} = 1.0 Wb.

From graphs presented in Figure 3 it can be stated that the relative difference between values of component u_{sy} and voltage magnitude U_s of stator voltage of induction generator does not exceed 10% at the wide range of changes of the stator current component i_{sx}.

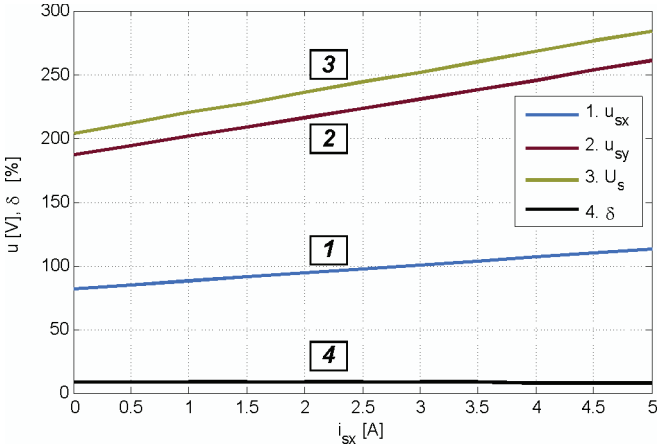

Fig. 3. Stator voltage vector component (u_{sx}, u_{sy}) and stator voltage vector magnitude U_s of induction generator and the relative error δ between voltage component u_{sy} and magnitude U_s for various values of stator current vector component i_{sx} and constant stator current vector component $i_{sy} = -3$ A

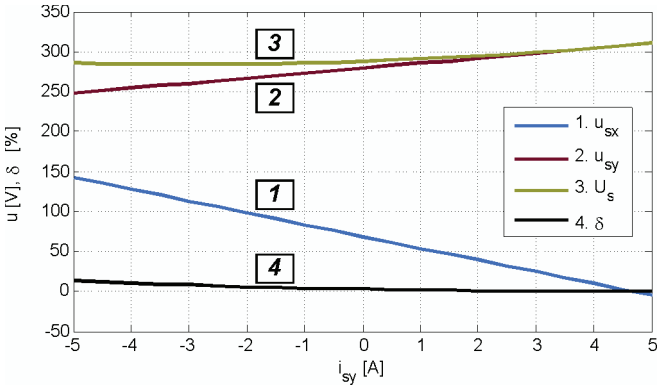

Fig. 4. Stator voltage vector component (u_{sx}, u_{sy}) and stator voltage vector magnitude U_s of induction generator and the relative error δ between voltage component u_{sy} and magnitude U_s for various values of stator current vector component i_{sy} and constant stator current vector component $i_{sx} = 5$ A

From graphs presented in Figure 4 results that the relative difference between component u_{sy} and voltage magnitude U_s also does not exceed 10%, during changes of the stator current component i_{sy}. The calculations show that for considered range of changes of the values of stator current components, the voltage component u_{sy} is approximately equal to the voltage magnitude U_s:

$$U_s = \sqrt{u_{sx}^2 + u_{sy}^2} \cong u_{sy}. \tag{14}$$

Assuming that the voltage drop across the stator phase resistance and the derivative of the vector flux of stator is negligible, after some manipulations of the equations (1) we obtain the following relationship:

$$\frac{u_{sy}}{i_{sx}} \cong K_r \frac{1}{1+T_r s}, \tag{15}$$

where: $K_r = \omega_\Psi L_M^2/L_r$, $T_r = L_r/R_r$, s – Laplace operator.

After using the Equations (14) and (15) the structure of the control system of stator voltage magnitude of induction generator has been synthesized and presented in Figure 5.

In this control structure the component i_{sx} of the stator current vector is controlled indirectly by forcing the suitable component i_{px} of converter current vector. On the base of the Equation (6) and after neglecting the voltage derivative component $\mathrm{d}u_{sx}/\mathrm{d}t$ in considered reference frame, we can assume that $i_{px} = i_{ox} - \omega_K C u_{sy} + i_{sx}$. After subtracting the component $C\omega_K u_{sy}$ from the command current i^*_{sx} the additional feedback to voltage regulator control loop will be introduced. In order to eliminate the possibility of voltage oscillations caused by this additional feedback, a sufficiently large time constant T_{zp} should be chosen, and therefore sufficiently small value of gain of the current controller K_{Rp} should be applied (Eq. (11)).

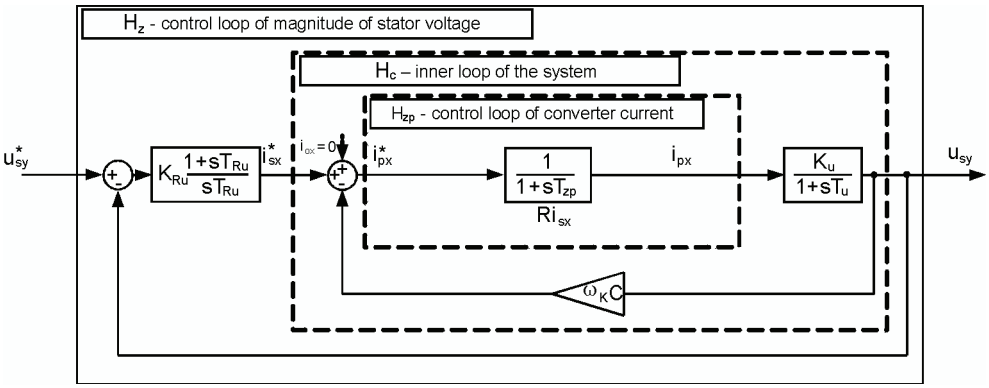

Fig. 5. Scheme of control system of inverter current i_{px} and voltage amplitude U_s

For the data: $\omega^2_\Psi = 314$ rad/s, $C = 1/(\omega^2_\Psi L_m) = 40$ μF, $K_r = 69$ V/A, $T_r = 77$ ms the minimum gain value K_{Rp} of the current regulator, for which the step response of the system described by transmittance $H_c(s)$ (Fig. 5) will have aperiodic character, is $K_{Rp} = 4.89$ V/A. The analysis of the current control system shows that the value of K_{Rp} can't be increased, because it may result in loss of the control, caused by the rapid discharge of the capacitor C_d in the DC link of the converter.

Figure 6 shows the equivalent scheme of the stator voltage control loop, after corresponding selection the parameters of the current control loop of the inverter. The gain parameter K_c of transfer function $H_c(s)$ is specified as follows:

$$K_c = \frac{K_u}{1+\omega_\Psi C}. \tag{16}$$

The internal control loop $H_c(s)$ is described by the second order transfer function with time constants T_{c1} and T_{c2} respectively, where $T_{c1} < T_{c2}$.

In order to compensate the larger time constant T_{c2} in transmittance $H_c(s)$, the integral time constant T_{Ru} of voltage control loop should be equal to the value of the larger time constant:

$$T_{Ru} = T_{c2}. \tag{17}$$

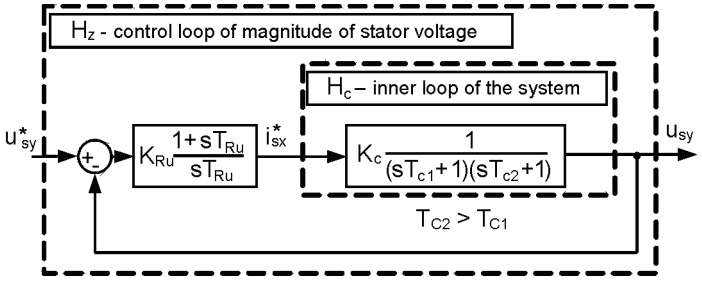

Fig. 6. Scheme of i_{px} current control of inverter and voltage amplitude U_s

The gain parameter K_{Ru} of voltage controller has been chosen in such a way that the values of poles of control system are not complex. Based on the performed calculations the following values of the voltage controller have been obtained: K_{Ru} = 0.0191 A/V, $T_{Ru} = T_{c2}$ = 34.6 ms. The smaller uncompensated time constant in this case is equal to T_{c1} = 12.2 ms.

Figure 7 shows the resultant transfer function of the voltage magnitude of induction generator.

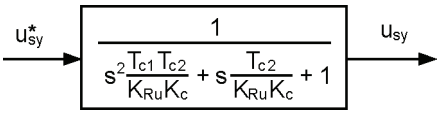

Fig. 7. Scheme of current control of inverter i_{px} and voltage amplitude U_s a) – resultant transmittance

3.3. Control of y-axis current component and DC link voltage of AC/DC converter

On the basis of the power balance between the AC circuit and DC circuit (neglecting losses in the AC/DC converter and the voltage drop across the resistance Rp), we can get the following relationship between the AC and DC circuits of the AC/DC converter:

$$i_d = \frac{p}{u_d} = \frac{3}{2}\frac{u_{px}i_{px} + u_{py}i_{py}}{u_d} \cong \frac{3}{2}\frac{u_{sx}i_{px} + u_{sy}i_{py}}{u_d}. \tag{18}$$

Taking into account that the component u_{sy} is much larger than component u_{sx} (Eq. (14)) and that the dynamics of control loop of current i_{px} and i_{py} is much larger than the dynamics of voltage control, Equation (18) can be simplified to the form:

$$i_d \cong \frac{3}{2}\frac{u_{sy}i_{py}}{u_d} = \frac{3}{2}mi_{py}, \tag{19}$$

where $m = u_{sy}/u_d$.

Based on Equations (4) and (19) the control structure of the DC link voltage u_d has been developed and depicted in Figure 8. In this system, the controller of i_{py} current component has been designed in the same manner as the controller of i_{px} current component. The gain of cur-

rent controller was selected so that the current control time of regulation was equal to $t_r = 75$ ms. Based on the performed calculations, the following values of the parameters of the i_{py} current controller were carried out: $K_{Rp} = 2.61$ V/A, $T_{Rp} = 250$ ms.

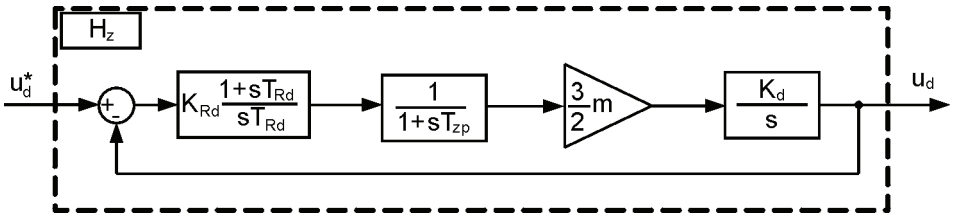

Fig. 8. Scheme of inverter current control i_{py} and direct voltage u_d ($K_d = 1/C_d$)

Because in the control system of DC link voltage the integral and the inertial element with small time constant exist, the symmetry criterion [3] has been used for tuning parameters of voltage control loop. As a result of the performed calculations, the following values of the voltage controller have been obtained: $K_{Rd} = 0.069$ A/V, $T_{Rd} = 77$ ms. Transfer function of the DC link voltage control loop is as follows:

$$H_z(s) = \frac{u_d}{u_d^*} = \frac{(sT_{Rp} + 1)}{\left(s^3 8T_{zp}^3 + s^2 8T_{zp}^2 + s4T_{zp} + 1\right)}. \tag{20}$$

In order to compensate the force element (numerator of $H_z(s)$ of transfer function the low pass filter $H_F(s)$ with a time constant T_F equal to time constant T_{Rd} has been used in control system, as shown in Figure 9. The resultant transfer function of DC link voltage control loop is equal to:

$$H_z(s) = \frac{u_d}{u_d^*} = \frac{1}{(s^3 8T_{zp}^3 + s^2 8T_{zp}^2 + s4T_{zp} + 1)}. \tag{21}$$

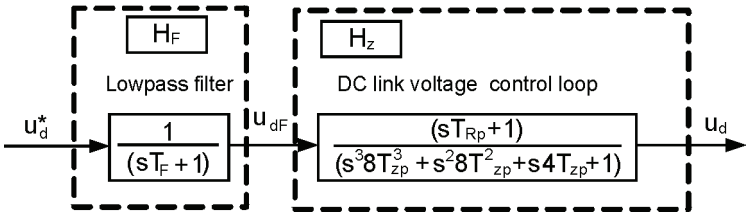

Fig. 9. DC link voltage control loop using a low pass filter element in order to compensate force element in voltage control circuit

4. Simulation results

Simulation studies of presented FOC methods used for control of induction generator have been performed. The studies have been carried out for 1.7 kW induction machine with two

pair of poles. Rated data of induction machine, used to study and simulation are the following: U_n = 220/380 V, P_n = 1700 W, f_n = 50 Hz, p_b = 3. Induction machine parameters were measured on experimental set-up. They are respectively: R_s = 3.57 Ω, R_r = 3.68 Ω, $L_{s\sigma}$ = 0.022 H, $L_{r\sigma}$ = 0.034 H, the coefficients of magnetizing function: A_m = 1.11 Vs, B_m = 0.289 1/A.

The selected results of simulation of DFOC control of rotor flux control have been presented in Figures 10 and 11.

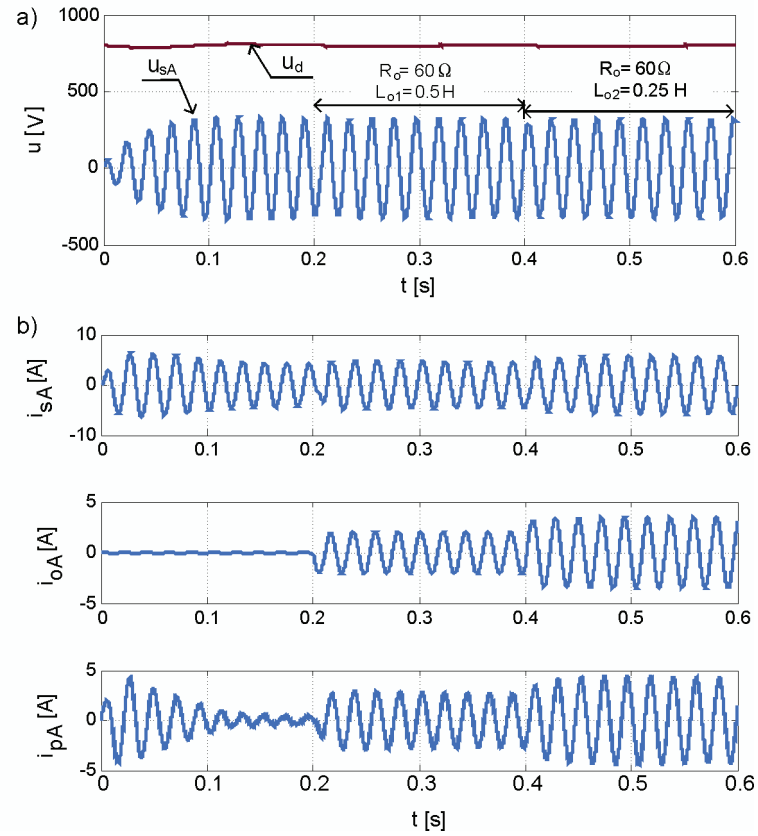

Fig. 10. Waveform during load of induction generator with active and reactive power

Figure 10a shows the waveforms of the instantaneous stator voltage of generator and the voltage in DC link of AC/DC inverter. Figure 10b presents the waveforms of stator current, load current and current of AC/DC converter respectively, during changing the load at time t = 0.2 s and t = 0.4 s. The simulation tests presented in Figure 10 shows that the control system maintains a constant amplitude of the stator voltage of the induction generator. As can be seen, even at a relatively low power factor of the load, the control system is able to stabilize the voltage at the terminals of the induction generator. The DC link voltage u_d of AC/DC converter is also maintained practically at constant value, during changes of the load.

From the waveform of AC/DC converter current presented in Figure 10 it can be stated, that the converter provides to the generator practically only reactive power. In addition, we can observe that the current of the inverter is practically equal to zero when the generator is no loaded. In this case all reactive power is delivered to the generator from the exciting capacitor bank.

Figure 11 shows the influence of changes of the rotor speed of the generator to the stabilization of stator voltage amplitude. It has been simulated that the rotor speed at first have the constant value, then from t = 0.2 s linear falls and from t = 0.6 linear rises. The performed simulations show, that the amplitude of stator voltage has practical constant value. The control system ensures, that the DC link voltage u_d is practically at the constant value, even during relatively fast changes in speed.

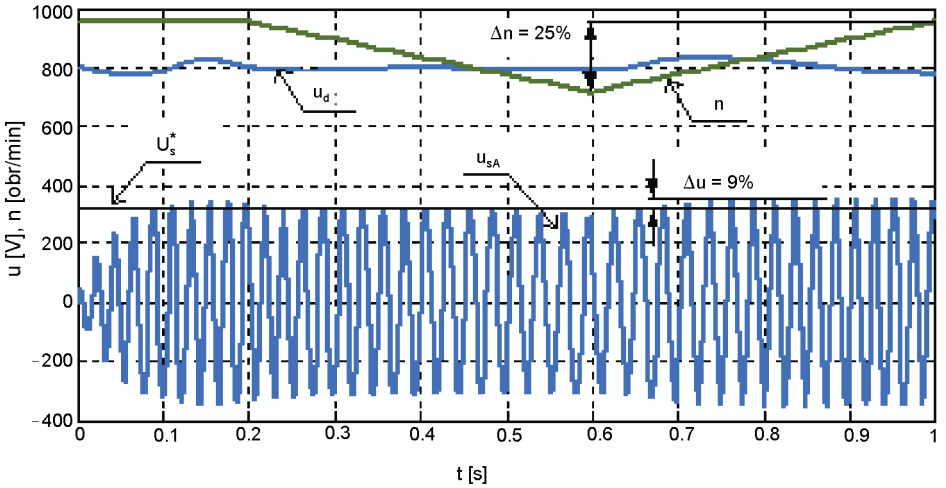

Fig. 11. Influence of changes the angular velocity of the generator rotor to voltage stabilization u_{SA} and u_d

5. Summary

This paper has provided an advanced control system of isolated induction generator with application of direct rotor field-oriented method of control. The presented control method of induction generator is reliable and quite simple. The system of autonomous induction generator with converter control system allows to stabilize the voltage amplitude of the generator and the DC link voltage of the converter AC/DC. The control system ensures the stabilization of the stator voltage amplitude of induction generator even at high dynamic load changes and changes of rotor speed of generator.

Additional exciting capacitor bank in the system enables to reduce the apparent power of the inverter. The AC/DC inverter in the steady states provides to the system of the generator and the load only reactive power.

The advantage of the presented control method is relatively simple way of the synthesis of the control system of the stator voltage amplitude and the voltage in DC link of AC/DC converter. But the disadvantage of this control method is the need of a precise estimation of rotor flux space vector and a large number of processed signals.

References

[1] Ahmed T., Nishida K., Nakaoka M., *Advanced Voltage Control of Induction GeneratorUsing RotorField-Oriented Control.* IAS 4: 2835-2842 (2005).
[2] Dong-Choon Lee, Jeong-Ik Jang, *Output voltage control of PWM inverters for stand-alone wind power generation systems using feedback linearization.* Industry Applications Conference 3: 1626-1631 (2005).
[3] Frohr F., Ortenburger F., *Einführung in die elektronische Regelungstechnik (Wprowadzenie do elektronicznej techniki regulacji).* Warszawa, WNT (1977).
[4] Idjdarene K., Rekioua D., Rekioua T., Tounzi A., *Control strategies for an autonomous induction generator taking the saturation effect into account.* European Conference on Power Electronics and Applications, pp.1-10 (2007).
[5] Jakubowski B., Pienkowski K., *Synthesis of the converter control system of autonomous induction generator. Part II-Simulation studies. (Synteza przekształtnikowego układu sterowania autonomicznym generatorem indukcyjnym. Część II – badania symulacyjne).* Prace Naukowe Instytutu Maszyn, Napędów i Pomiarów Elektrycznych 32: 85-91,Wrocław (2012) (in Polish).
[6] Jakubowski B., Pienkowski K., *Analysis of field-oriented control systems of isolated self-excited induction generator. (Analiza układów polowo-zorientowanego sterowania autonomicznym generatorem indukcyjnym).* Electrical Review (Przegl. Elektrot.) 87(11): 111-115 (2011) (in Polish).
[7] Murthy S.S., Bhuvaneswari G., Gao S., Gayathri M., *Performance Analysis of a Self Excited Induction Generator with Digitally Controlled Electronic Load Controller for Micro Hydel Power Generation.* POWERCON, pp. 1-6 (2008).
[8] Nesba A., Ibtiouen R., Mekhtoub S et al., *Analysis of self-excited induction generator feeding DC loads for low-cost renewable energy applications*. IEMDC, pp. 812-817 (2009).
[9] Pienkowski K., *Induction Generator With PWM-Inverter Excitation.* Proceedings of XVI Sympodium on Electromagnetic Phenomena in Nonlinear Circuits, Cracow, Poland, pp. 123-126 (2000).
[10] Silva S.R., Lyra R.O.C., *PWM converter for excitation of induction generators.* Proc. of Fifth European Conference on Power Electronics and Applications, Brighton, UK, 8: 174-178 (1993).
[11] Seyoum D., Rahman M.F., Grantham C., *Terminal voltage control of a wind turbine driven isolated induction generator using stator oriented field control.* APEC'03, 2: 846-852 (2003).